Polyhedron 30 (2011) 340–346

Contents lists available at ScienceDirect

Polyhedron

journal homepage: www.elsevier.com/locate/poly

Mononuclear transition metal complexes with sterically hindered carboxylate ligands: Synthesis, structural and spectral properties

Sethuraman Kannan [a], Galmari Venkatachalam [a], Ha-Jin Lee [b], Byoung Koun Min [c], Woong Kim [d], Eunhae Koo [e], Young Rag Do [a], Sungho Yoon [a,*]

[a] Department of Chemistry, Kookmin University, 861-1 Jeoungnung-dong, Seongbuk-gu, Seoul 136-702, Republic of Korea
[b] Jeonju Center, Korea Basic Science Institute, 664-14 Dukjindong-1-ga, Dukjin-gu, Jeonju 561-756, Republic of Korea
[c] Department of Clean Energy Research Center, Korea Institute of Science and Technology, 39-1 Hawolgok-dong, Seongbuk-gu, Seoul 136-791, Republic of Korea
[d] Department of Materials Science and Engineering, Korea University, Seoul 136-713, Republic of Korea
[e] Bio-IT Convergence Center, Korea Institute of Ceramic Engineering and Technology, Seoul, Republic of Korea

ARTICLE INFO

Article history:
Received 28 May 2010
Accepted 28 October 2010
Available online 5 November 2010

Keywords:
Mononuclear metal complexes
Sterically hindered carboxylate ligand
3,5-Dimethylpyrazole
Crystal structures

ABSTRACT

The metal coordination geometry in the active site of metalloproteins are very different from the one of small inorganic complexes, due to the inflexibility of the ligand set from amino acid side chains different from freely moving ligand set in synthesis. Using the sterically hindered 2,6-di-(*p*-fluorophenyl)benzoate(L) ligand, a series of mononuclear Co(II), Ni(II) and Cu(II) complexes of general formula $[M(L)_2(Hdmpz)_2]$ (where, Hdmpz = 3,5-dimethyl pyrazole) have been synthesized and characterized by the variety of spectroscopic methods. A distorted octahedral geometry in case of nickel, tetrahedral geometry for cobalt and square pyramidal in copper was observed in the X-ray studies, which also revealed that the uncoordinated oxygen atom of the carboxylate group forms intramolecular hydrogen bonding with the N–H group of the coordinated 3,5-dimethylpyrazole in case of cobalt and copper.

1. Introduction

The research on the metal carboxylates has always been intriguing in that they play important roles not only in synthetic chemistry with the essence of labile coordination modes of carboxylate group, such as architecture of open and porous framework [1,2], but also in biologic activities [3,4] and physiological effects [5,6]. A versatile carboxylate anion can adopt a wide range of bonding modes, including monodentate, symmetric and asymmetric chelating, and bidentate and monodentate bridging [7]. It is generally known that the carboxylate complexes of the 3*d* elements in active sites of enzymes play an important role in redox chemistry. For example, metal active sites catalyze fundamental transformations such as the conversions of oxygen to water, water to oxygen, nitrogen to ammonia and methane to methanol. Because the behavior of metal ions in proteins cannot be divorced from the fundamental chemistry of the particular metal, the study of small molecule, active-site synthetic analogs is useful [8,9]. Synthetic models with carboxylates, imines and thiolates as the ligands are exploited in order to sharpen or focus certain questions related to the role of metals in metalloenzymes [10–12]. The goal is to elucidate fundamental aspects of structure, spectroscopy, magnetic and electronic structure, reactivity and chemical mechanism. The biological functions of some selected metal ions like copper, iron, cobalt manganese and nickel have undergone an extensive research but the quest for more advancement still exists. We have focused on cobalt, nickel and copper mononuclear complexes of the carboxylate ligand with a potential to expand the understanding of the coordination chemistry and substrate binding in enzymes with these metal active sites.

A common structural feature found in most of the metalloproteins and enzymes is the presence of one or more carboxylate groups derived from aspartate or glutamate side chains of the protein. The carboxylate group of glutamate and aspartate works as supporting ligand for the metal center in various metalloproteins and behave as monodentate or bidentate depending upon the requirement of active site. Besides vitamin B_{12} which catalyses the *trans*-alkylation and isomerization reactions *via* Co(III)-alkyl intermediate [13], there are several other cobalt containing proteins and enzymes such as ribonucleotide reductase (RR), MAPs (methionine aminopeptidases), glucose isomerases, cobalt transporters, bromoperoxidase, etc. where cobalt plays directly or indirectly an important role [14]. Similarly, copper-containing oxidases and oxygenases comprise a large class of enzymes containing varying numbers of copper ions having diverse structures. The organic cofactors in copper-containing amine oxidases (AO) and lysyl oxidase (LO), dopamine β-monooxygenase (DβM) and peptidylglycine α-hydroxylating monooxygenase (PHM) all involves mononuclear copper active-oxygen species [15–17].

---

* Corresponding author. Tel.: +82 2 910 4763; fax: +82 2 910 4415.
E-mail address: yoona@kookmin.ac.kr (S. Yoon).

0277-5387/$ - see front matter Crown Copyright © 2010 Published by Elsevier Ltd. All rights reserved.
doi:10.1016/j.poly.2010.10.019

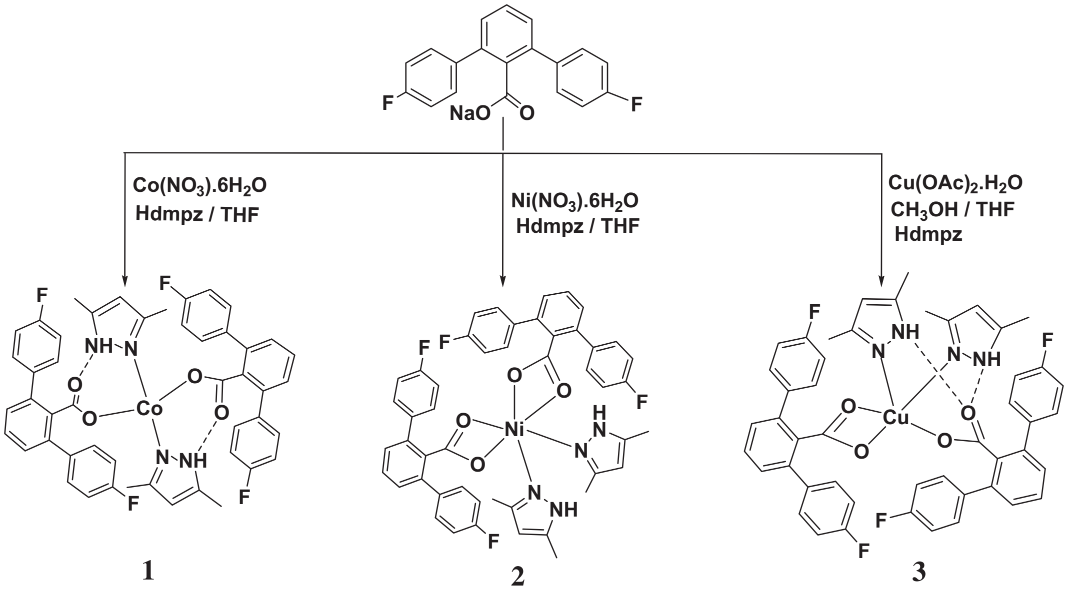

Scheme 1. General reaction scheme for synthesis of metal complexes.

The literature also show that dinuclear nickel complexes with bridging carboxylates [18,19] are interesting for their magnetic interactions, whereas the mononuclear complexes play an important role in modeling the active site of metalloproteins [2,20–22]. With nickel(II) as its native metal ion, urease catalyses the hydrolysis of urea to ammonia and carbamate and in turn spontaneous decomposition of CO_2 and a second molecule of ammonia [23]. However structurally characterized nickel carboxylate complexes are limited in literature [24,25].

Ever since, the simultaneous recognition of Lippard and Tolman that sterically hindered *m*-terphenyl carboxylates were ideal ligands for the preparation of model compounds of the enzyme active site of non-heme diiron enzymes [26,27], several reports on the use of this class of sterically hindered *m*-terphenyl ligands for diiron enzymes as well as copper and manganese enzymes have appeared in the literature which involves the dinuclear metal carboxylates [28,29]. Lee et al. also reported the carboxylate bridged dinuclear cobalt and nickel complexes of sterically hindered 2,6-di(p-tolyl)benzoic acid as a model of metallohydrase active sites [30]. However, mononuclear copper(II), cobalt(II) and nickel(II) complexes of this class of ligands are rarely reported [31,32]. Herein, we report the synthesis and characterization of mononuclear cobalt, nickel and copper complexes incorporating the sterically hindered terphenyl carboxylate ($^{-}O_2CAr^{4\text{-}FPh}$) and 3,5-dimethylpyrazole (Hdmpz) as a co-ligand (Scheme 1).

2. Experimental

2.1. General considerations

All chemicals purchased were of analytic grade and were used without further purification. All reactions were carried out under N_2 atmosphere by using Schlenk techniques. FT-IR spectra were recorded using Varian 640-IR FT-IR spectrometer. UV–Vis spectra were recorded on a OPTIZEN 2120UV spectrophotometer. Electrochemical studies were performed using a Zahner Elektrik IM 6 model potentiostat with 0.5 M dichloromethane solutions of $[(n\text{-}C_4H_9)_4N]PF_6$ as supporting electrolyte under a nitrogen atmosphere. A three-electrode configuration consisting of a platinum working electrode, a platinum wire auxiliary electrode and an Ag/AgCl reference electrode.

2.2. Preparation of $NaO_2CAr^{4\text{-}FPh}$

The *m*-terphenyl carboxylate ligand 2,6-di-(*p*-fluorophenyl)-benzoate) ($HO_2CAr^{4\text{-}FPh}$) was prepared according to literature procedures [33–35]. The sodium salt of the carboxylic acid ($NaO_2CAr^{4\text{-}FPh}$) was prepared by treating a MeOH solution of the free acid with 1 equiv. of NaOH and removing the volatile fractions under reduced pressure.

2.3. Synthesis of complexes

2.3.1. Preparation of $[Co(O_2CAr^{4\text{-}FPh})_2(Hdmpz)_2]$ (**1**)

To a 20 mL THF solution of $Co(NO_3)_2{\cdot}6H_2O$ (0.25 mmol; 0.072 g) was added (0.42 mmol; 0.17 g) of $NaO_2CAr^{4\text{-}FPh}$ and the reaction mixture was stirred for 5 h under N_2. To this reaction mixture, 3,5-dimethylpyrazole (0.50 mmol; 0.048 g) abbreviated as Hdmpz was added and stirring was continued for overnight. The volatile fractions were removed under reduced pressure and extracted with CH_2Cl_2 and filtered to remove any undissolved solid. Violet blocks of **1** suitable for X-ray diffraction were obtained by vapor diffusion of pentane into the dichloromethane solution. Yield: 0.050 g (46% based on Co). FT-IR (NaClr, cm^{-1}): 2961(w), 2927(w), 2341(s), 2359(m), 1606(s), 1562(s), 1510(s), 1456(m), 1409(m), 1367(s), 1288(m), 1222(s), 1159(s), 1048(s), 1015(w), 843(m), 809(m), 793(w), 738(m), 705(m), 556(m), 534(m). UV–Vis (CH_2Cl_2) (λ_{max}, nm (ε, $M^{-1}\ cm^{-1}$)): 533 (342), 568 (441), 592 (410). *Anal.* Calc. for $C_{48}H_{38}F_4N_4CoO_4$: C, 66.28; H, 4.40; N, 6.44. Found: C, 66.40; H, 4.88; N, 6.60%.

2.3.2. Preparation of $[Ni(O_2CAr^{4\text{-}FPh})_2(Hdmpz)_2]$ (**2**)

Compound **2** was synthesized in a manner similar to that of **1** with $Ni(NO_3)_2{\cdot}6H_2O$ as the starting metal salt. Light green single crystals suitable for X-ray diffraction were obtained by vapor diffusion of pentane into the dichloromethane solution. Yield: 0.110 g (50% based on Ni). FT-IR (NaCl, cm^{-1}): 3397(s), 2925(m), 2856(w), 2359(m), 2341(w), 1652(w), 1596(m), 1558(s), 1540(s), 1511(s), 1456(s), 1410(m), 1380(s), 1281(w), 1223(s), 1159(s), 1039(w), 838(s), 811(s), 792(s), 731(m), 704(m), 582(w), 555(m), 530(m), 473(w), 461(m). UV–Vis (CH_2Cl_2) (λ_{max}, nm (ε, $M^{-1}\ cm^{-1}$)): 419 (51), 685 (21), 785 (13). *Anal.* Calc. for $C_{48}H_{38}F_4N_4NiO_4$: C, 66.30; H, 4.40; N, 6.64. Found: C, 66.70; H, 5.00; N, 6.60%.

2.3.3. Preparation of [Cu($O_2CAr^{4\text{-}FPh}$)$_2$(Hdmpz)$_2$] (**3**)

To a 10 mL solution of of $HO_2CAr^{4\text{-}FPh}$ (0.50 mmol; 0.077 g) in methanol, was added Cu(II) acetate monohydrate (0.25 mmol; 0.050 g) and the reaction mixture was stirred for 15 min. To this reaction mixture, Hdmpz (0.50 mmol; 0.048 g) was added. The color of the solution changed to green and THF (10 mL) was added to ensure complete dissolution. Stirring was continued for another 3 h. Green crystals of **3** suitable for X-ray diffraction were obtained by slow evaporation. Yield: 0.095 g (44% based on Cu). FT-IR (NaCl, cm^{-1}): 3367(br,w), 3226(br,w), 3057, 3042, 2927, 2605, 2513, 1606, 1552, 1511, 1454, 1407, 1379, 1298, 1222, 1159, 1095(w), 1047(w), 838, 809, 792, 769, 730, 554, 531, 490, 475, 461. UV–Vis (CH_2Cl_2) (λ_{max}, nm (ε, $M^{-1}\,cm^{-1}$)): 755 (73). *Anal.* Calc. for $C_{48}H_{38}F_4N_4CuO_4$: C, 65.93; H, 4.38; N, 6.41. Found: C, 66.82; H, 4.82; N, 6.42%.

2.4. X-ray crystallographic studies

Single crystals were mounted at room temperature on the tips of quartz fibers, coated with Partone-N oil, and cooled under a stream of cold nitrogen. Intensity data were collected on a Bruker CCD area diffractometer running the SMART software package, with Mo Kα radiation (λ = 0.71073 Å). The structures were solved by direct methods and refined on F^2 by using the SHELXTL software package [36]. Empirical absorption corrections were applied with SADABS [37], part of the SHELXTL program package, and the structures were checked for higher symmetry by the program PLATON [38]. All non-hydrogen atoms were refined anisotropically. In general, hydrogen atoms were assigned idealized position and given thermal parameters equivalent to 1.2 times the thermal parameter of the carbon atom to which they are attached. Data collection and experimental details for the complex are summarized in Table 1 and relevant interatomic distances and angles are listed in Table 2.

Table 1
Summary of X-ray crystallographic data for [Co($O_2CAr^{4\text{-}FPh}$)$_2$(Hdmpz)$_2$](**1**), [Ni($O_2CAr^{4\text{-}FPh}$)$_2$(Hdmpz)$_2$](**2**), and [Cu($O_2CAr^{4\text{-}FPh}$)$_2$(Hdmpz)$_2$](**3**).

	1	**2**	(**3**)$_4$·CH_3OH
Empirical formula	$C_{48}H_{36}CoF_4N_4O_4$	$C_{48}H_{38}F_4N_4NiO_4$	$C_{193}H_{156}Cu_4F_{16}N_{16}O_{17}$
Formula weight	867.74	869.53	3529.50
Space group	$P\bar{1}$	C_2/c	$P2_1/n$
a (Å)	11.1281(12)	26.839(5)	18.4779(3)
b (Å)	13.7586(13)	8.2580(16)	10.8361(2)
c (Å)	15.5806(16)	20.067(4)	21.7164(4)
α (°)	68.788(2)		
β (°)	88.767(2)	110.809(3)	101.5940(10)
γ (°)	77.525(3)		
V (Å^3)	2167.2(4)	4157.4(14)	4259.52(13)
Z	2	4	1
D_{calc}, (g/cm^3)	1.330	1.389	1.376
T (K)	296(2)	173(2)	296(2)
Absorption coefficient (mm^{-1})	0.461	0.535	0.581
Total number of data	16286	17270	22710
Number of unique data points	10601	4824	4422
Number of parameters	554	282	582
R_1 (%)[a]	7.29	3.45	3.71
wR_2 (%)[b]	12.67	9.31	6.24
Largest difference in peak and hole (e Å^{-3})	0.464 and −0.536	0.394 and −0.342	0.238 and −0.352

[a] $R_1 = \Sigma||F_o| - |F_c||/\Sigma|F_o|$.

[b] $wR_2 = \{\Sigma[w(F_o^2 - F_c^2)^2]/\Sigma[w(F_o^2)^2]\}^{1/2}$.

Table 2
Selected inter-atomic distances (Å) and angles (°) for [Co($O_2CAr^{4\text{-}FPh}$)$_2$(Hdmpz)$_2$] (**1**)[a].

Inter-atomic distance	
Co(1)–O(1)	1.943(3)
Co(1)–O(3)	1.968(3)
Co(1)–N(1)	2.037(4)
Co(1)–N(3)	2.009(4)
Co(1)···O(2)	2.959(3)
Co(1)···O(4)	3.076(4)
O(4)···N(4)	2.778(4)
O(2)···N(2)	2.698(4)
Inter-atomic angles	
O(1)–Co(1)–O(3)	112.08(14)
O(1)–Co(1)–N(3)	108.25(14)
O(3)–Co(1)–N(3)	108.88(14)
O(1)–Co(1)–N(1)	114.59(15)
O(3)–Co(1)–N(1)	101.84(14)
N(3)–Co(1)–N(1)	111.02(17)

[a] Numbers in parentheses are estimated standard deviations of the last significant figures.

3. Results and discussion

3.1. Rationale for the synthetic approach

The use of pyrazole or pyrazole derivatives has drawn strong interest in modeling biological systems. Trofimenko has used pyrazole in polypyrazolyborates to stabilize a variety of organometallic and coordination complexes [39] which are valuable in biomimetic coordination chemistry of numerous metalloproteins since these monoanionic, facially coordinating ligands have histidine-like donors which can hold three *cis* sites fixed while leaving other coordination sites open. Thus, a variety of complexes with 3,5-dimethylpyrazoles have been synthesized and employed in coordination and organometallic chemistry [40–42]. To the best of our knowledge direct synthesis of mononuclear transition metal complexes of 2,6-di(4-fluorophenyl)benzoate) ($HO_2CAr^{4\text{-}FPh}$) containing 3,5-dimethylpyrazole as co-ligand have not been reported. The synthesis of the mononuclear complexes were achieved *via* the reaction of metal salts, carboxylate ligand and 3,5-dimethylpyrazole in 1:2:2 M ratio. The complexes were characterized by IR, UV–Vis spectral techniques. The coordination modes are different in all three cases as evidenced by single crystal diffraction studies. The characteristic bands of carboxylate groups are shown in the range of 1540–1606 cm^{-1} for asymmetric stretching and 1407–1456 cm^{-1} symmetric stretching [43], respectively. The absence of any bands in the area of 1710 cm^{-1} indicates full deprotonation of all carboxylate groups in **1**–**3** [44], which is consistent with the results of the X-ray analysis.

3.2. Synthesis and characterization of [Co($O_2CAr^{4\text{-}FPh}$)$_2$(Hdmpz)$_2$] (**1**)

The reaction of the terphenyl carboxylate ligand with cobalt(II) nitrate hexahydrate in THF with 3,5-dimethylpyrazole, gives complex **1** with a square planar geometry around Co(II) ion (Fig. 1). The selected bond lengths and bond angles are given in Table 2. Both the carboxylic acid groups are deprotonated, necessitating a 1:2 metal:ligand ratio in the neutral compound. The two pyrazoles are present in *trans* conformation across a crystallographic mirror plane. The deprotonated pocket carboxylates are also *trans* and bound to the cobalt ions through a single oxygen, giving the metal tetrahedral geometry with O–Co–N angles of 108.34 and 114.77. The Co1–O1 and Co1–O3 bond distances are 1.943(3) Å and

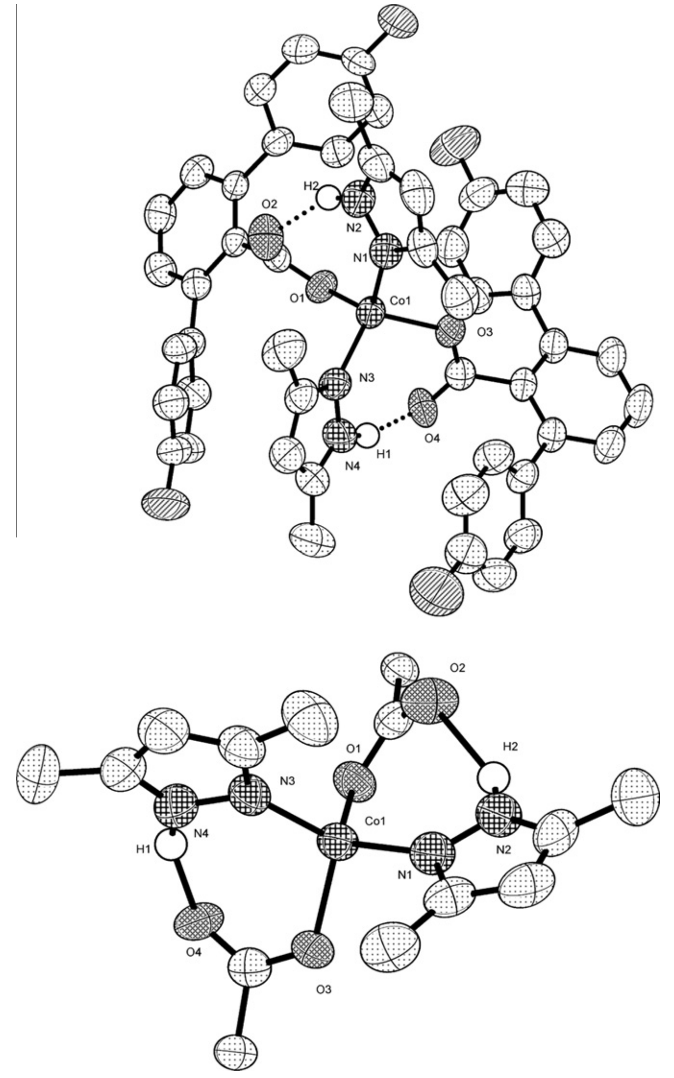

Fig. 1. Ortep drawing of $[Co(O_2CAr^{4\text{-}FPh})_2(Hdmpz)_2]$ (**1**) showing 50% probability thermal ellipsoids. The hydrogen atoms and the phenyl rings of $Ar^{4\text{-}FPh}COO^-$ ligand are omitted for clarity.

1.968(3) Å respectively, whereas Co1–O2 and Co1–O4 bond distances are 2.959(3) Å and 3.076(4) Å, respectively. The long distances for Co1–O2 and Co1–O4 indicated that these oxygens were not involved in bond formation with metal center. Two hydrogen-bonding interactions are observed between the carboxylate and Hdmpz ligands, the O···H–N distances being 2.778 and 2.698 Å. The electronic spectrum of cobalt complex (Fig. 2a) in dichloromethane shows a multicomponent absorptions with a resolved peak at 568 nm ($\varepsilon = 342\ M^{-1}\ cm^{-1}$) and two shoulders at 533 nm ($\varepsilon = 441\ M^{-1}\ cm^{-1}$) and 592 nm ($\varepsilon = 410\ M^{-1}\ cm^{-1}$) which definitely resulted from $^4A_2 \rightarrow {}^4T_1$ characteristic of Co(II) complexes [45]. Such weak absorption bands in the range of 550–700 nm, has been reported for d^7 Co(II) ions in methionine aminopeptidases (MAPs) [46].

3.3. Synthesis and characterization of $[Ni(O_2CAr^{4\text{-}FPh})_2(Hdmpz)_2]$ (2)

Compound **2** was synthesized by reaction of $Ni(NO_3)_2{\cdot}6H_2O$ with $NaO_2CAr^{4\text{-}FPh}$ in THF solution followed by treatment with 3,5-dimethylpyrazole in a 1:2:2 M ratio although analogous to preparation of complex **1**, affording a six coordinated mononuclear nickel complex **2**. The molecular structure of the complex **2** with the atom numbering scheme is illustrated in Fig. 3, and selected bond lengths and bond angles are given in Table 3. One coordination environment present in the asymmetric unit involves the coordination of Ni(II) ions by four oxygen atoms from two terphenyl carboxylate ligands in chelating bidentate modes and two nitrogen atoms from Hdmpz groups that are oriented *cis* to each another. The O2–Ni–O4 bite angle of the carboxylate in complex **2** is 104.77. One of the Ni–O1 bond distances is 2.193 Å whereas the other Ni–O2 is 2.040 Å reflecting the asymmetric binding of the carboxylate ligands. The difference of at least 0.018 Å for the M–O bond and 0.027 Å for the M–N bond may be due to the increased steric hindrance around the six-coordinate nickel compared to the four-coordinate cobalt in **1**. Thus, the complex **2** has axially elongated octahedral geometry around the Ni(II) cation. Compared with complex **1**, the oxygen atoms of the carboxylate ligand did not form intramolecular hydrogen bonding with N–H group of Hdmpz.

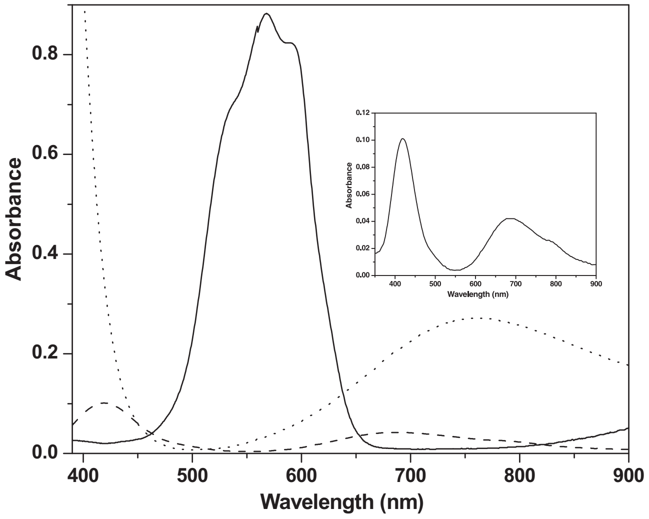

Fig. 2. UV–Vis spectra for (a) $[Co(O_2CAr^{4\text{-}FPh})_2(Hdmpz)_2]$ (**1**) (solid line); (b) $[Ni(O_2CAr^{4\text{-}FPh})_2(Hdmpz)_2]$ (**2**) (dashed line) and (c) $[Cu(O_2CAr^{4\text{-}FPh})_2(Hdmpz)_2]$ (**3**) (dotted line) in CH_2Cl_2. Inset shows the UV–Vis spectrum of the complex **2**.

This asymmetric binding is small when compared to iron mononuclear complex incorporating a sterically hindered terphenyl carboxylate ligand reported by Tolman et al. [47] and some other reports on similar binding of zinc and copper mononuclear complexes containing carboxylate ligands [48]. Complex **2** showed two peaks (Fig. 2b) at 419 nm ($\varepsilon = 51\ M^{-1}\ cm^{-1}$) and 685 nm ($\varepsilon = 21\ M^{-1}\ cm^{-1}$) caused by $^3A_{2g} \rightarrow {}^3T_{1g}(P)$ and $^3A_{2g} \rightarrow {}^3T_{1g}(F)$ transitions respectively and a weak absorption band at 785 nm ($\varepsilon = 13\ M^{-1}\ cm^{-1}$) is due to the spin-forbidden $^3A_{2g} \rightarrow {}^1E_{1g}$ transition in the electronic spectrum recorded in dichloromethane. This pattern of UV–Vis spectra of nickel complex further supports the octahedral geometry around Ni(II) ion [8,9].

3.4. Synthesis and characterization of $[Cu(O_2CAr^{4\text{-}FPh})_2(Hdmpz)_2]$ (3)

Treatment of the copper(II) acetate monohydrate and the terphenyl carboxylate ligand in methanol followed by 3,5-dimethylpyrazole (Hdmpz) leads to the formation of five coordinated mononuclear complex **3** in which one carboxylate is monodentate, the other is in a chelating bidentate mode, and the pyrazoles are *cis*-coordinated. The unsymmetric bidentate chelating mode of one of the carboxylate is supported by the difference in Cu1–O3 and Cu1–O4 bond distances. The ortep view of the crystal structure is shown in Fig. 4, and selected bond lengths and bond angles are given in Table 4. The stereochemistry of the copper center can be

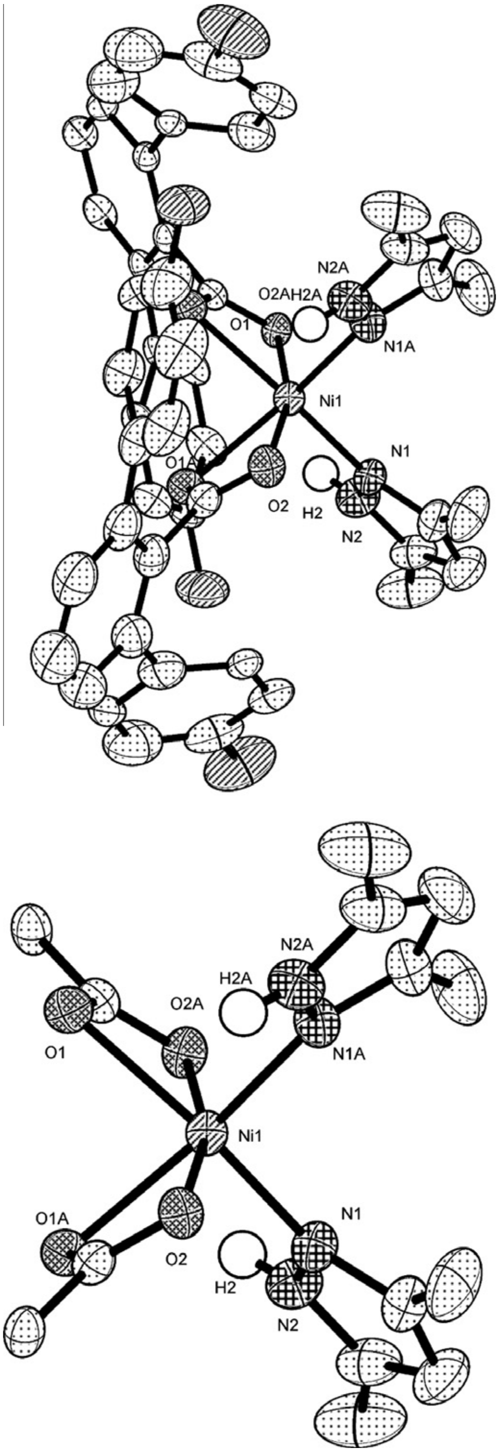

Fig. 3. Ortep drawing of $[\mathrm{Ni}(\mathrm{O_2CAr^{4\text{-}FPh}})_2(\mathrm{Hdmpz})_2]$ (**2**) showing 50% probability thermal ellipsoids. The hydrogen atoms and the phenyl rings of $\mathrm{Ar^{4\text{-}FPh}COO^-}$ ligand are omitted for clarity.

Table 3
Selected inter-atomic distances (Å) and angles (°) for $[\mathrm{Ni}(\mathrm{O_2CAr^{4\text{-}FPh}})_2(\mathrm{Hdmpz})_2]$ (**2**)[a].

Inter-atomic distance	
Ni(1)–O(1)	2.1929(10)
Ni(1)–O(2)	2.0403(10)
Ni(1)–N(1)	2.0194(12)
O(2)···N(2A)	3.0425(13)
Inter-atomic angles	
O(1)–Ni(1)–N(1)	152.66(4)
N(1)–Ni(1)–N(1A)	100.87(7)
O(2)–Ni(1)–N(1)	92.77(4)
O(1)–Ni(1)–N(1A)	97.37(4)
O(2)–Ni(1)–O(1)	104.77(4)

[a] Numbers in parentheses are estimated standard deviations of the last significant figures.

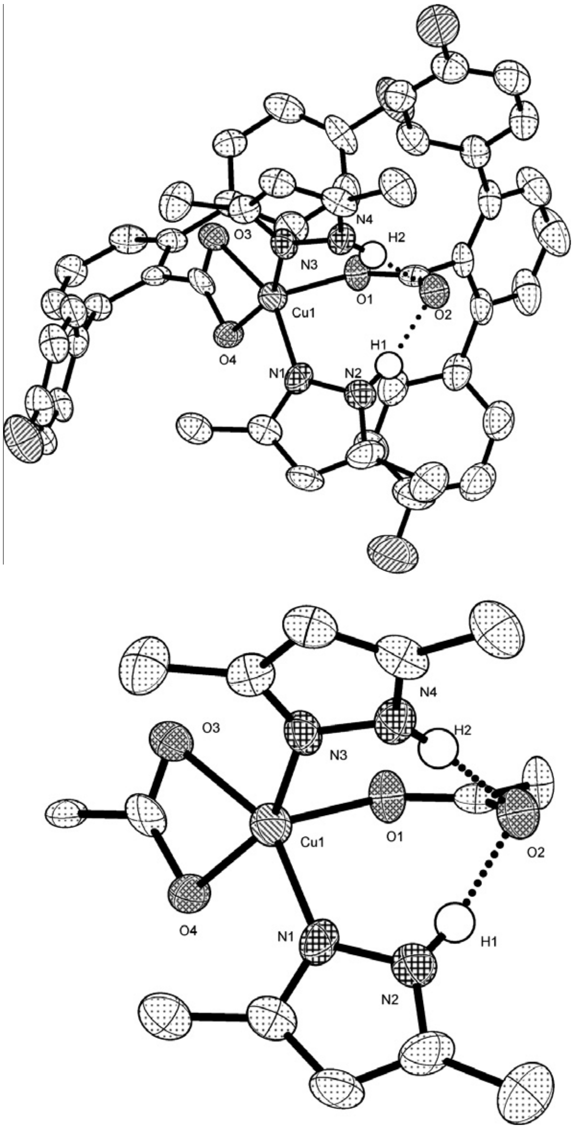

Fig. 4. Ortep drawing of $[\mathrm{Cu}(\mathrm{O_2CAr^{4\text{-}FPh}})_2(\mathrm{Hdmpz})_2]$ (**3**): left; showing 50% probability thermal ellipsoids. Structure with the phenyl rings of $\mathrm{Ar^{4\text{-}FPh}COO^-}$ ligand are omitted for clarity: right. The hydrogen atoms in the N–H group of Hdmpz ligands are added to show the hydrogen bonding interaction.

determined by the Addison τ factor, a parameter that describes the distortion from regular square pyramidal or trigonal bipyramidal [49]. In a regular square pyramidal, $\tau = 0$, and for a perfect trigonal bipyramidal $\tau = 1$. The coordination environment of the copper is a perfect square pyramidal with τ factor of 0.04. The two oxygen atoms of the bidentate carboxylate (O3 and O4) with the bite angle of 64.43° and the two coordinated nitrogen atoms (N1 and N3) of the pyrazole constitute the basal plane of the square pyramidal structure and the apical position is fulfilled by the oxygen atom (O1) of the monodentate carboxylate ligand. The apical Cu–O1 distance 2.109(6) Å is distinctly longer than the other coordinated oxygens of the carboxylate group comprising the basal plane as expected for the square pyramidal geometry of the copper chelate. Similar, to the cobalt complex **1** the Cu1–O1, Cu1–O3 and Cu1–O4 bond distances are 2.109(6) Å, 2.061(10) Å and 2.030(10) Å respectively are shorter than Cu1–O2 bond distance of 3.449(9) Å, which confirms the non-bonding of O2 with the metal center. This uncoordinated oxygen O2 exhibits intramolecular hydrogen bonding with the N–H group of the pyrazole moiety, with O2···N2 and O2···N4 interatomic distances of 2.754 and 2.821 Å, respectively. The electronic spectra of the copper complex **3** (Fig. 2c) recorded in dichloromethane solution, displayed a broad band centered at 749 nm ($\varepsilon = 73\ \mathrm{M^{-1}\,cm^{-1}}$) arising from $^2E_g \rightarrow {}^2T_{2g}$ transition, showing the characteristic feature of Cu(II) ions.

Because mononuclear iron(II) complexes with the sterically bulky carboxylates also been reported [50], the geometrical preference in a series of 3rd transition metal ions with sterically hindered coordination sphere was induced based on the structures in Scheme 2. The combined influence of the sterically hindered carboxylate ligands and the intramolecular hydrogen-bonding interactions changes the binding mode of the carboxylate ligands from monodentate to bidentate and stabilizes Fe(II) and Co(II) complexes, [Fe($O_2CAr^{4\text{-}FPh}$)$_2$(Hdmpz)$_2$] and **1**, with the low coordination number of 4.

3.5. Electrochemical properties of the complexes

Out of curiosity to determine the redox property of the complexes, the electrochemical experiments were studied in dichloromethane solution by cyclic voltammetry under N_2 atmosphere using a platinum working electrode and the redox potentials are expressed with reference to Ag/AgCl.

The cyclic voltammograms for the **1** and **2** complexes in CH_2Cl_2 between 1.5 and −1.5 V shows one irreversible reduction peak at −1.166 V and −0.319 V versus Ag/AgCl for cobalt and nickel, respectively. The representative cyclic voltammograms of cobalt and nickel are given in Fig. S1 in the supporting information. Repeated scans between 0.0 and −1.5 V showed a gradual decrease in current both in case of complex **1** and **2** demonstrating the irreversibility. The reason for the irreversibility observed for the reductive response of the complexes may be due to a short lived reduced state of the metal ion or due to oxidative degradation of the ligands. As compared with the nickel(II) complex, the cobalt(II) complex has more negative metal centered reduction, that means the metal centered reduction is more difficult to achieve in case of cobalt than nickel. The electrochemical processes in both nickel and cobalt are metal centered as the ligand shows no peak in the potential window scanned for the complexes. Copper(II) mononuclear complex **3** exhibit an electrochemically quasi-reversible oxidation (Cu^{II}/Cu^{III}) at 0.317 V versus Cp_2Fe^+/Cp_2Fe with $\Delta E_p = 103$ mV with scan rate of 100 mV/s. Even with a scan rate of 250 mV/s the redox couple remained quasi-reversible. Upon the positive scan towards the cathodic potential the copper complex shows an oxidation peak and only a small reduction peak (Fig. 5). In case of copper chelate also we notice a decrease in the anodic and cathodic current during the second cycle. Further scanning toward either more positive or more negative potential within the solvent potential window indicated the absence of redox activity.

Table 4
Selected inter-atomic distances (Å) and angles (°) for [Cu($O_2CAr^{4\text{-}FPh}$)$_2$(Hdmpz)$_2$] (**3**)[a].

Interatomic distance	
Cu(1)–O(1)	2.109(6)
Cu(1)–N(1)	1.980(10)
Cu(1)–N(3)	1.964(10)
Cu(1)–O(3)	2.061(10)
Cu(1)–O(4)	2.030(10)
Cu(1)···O(2)	3.449(9)
O(2)···N(2)	2.754(10)
O(2)···N(4)	2.821(10)
Interatomic angles	
O(1)–Cu(1)–N(1)	99.47(4)
O(1)–Cu(1)–N(3)	98.16(4)
N(1)–Cu(1)–N(3)	98.33(5)
O(1)–Cu(1)–O(3)	96.97(5)
O(1)–Cu(1)–O(4)	96.00(1)
O(3)–Cu(1)–O(4)	64.43(11)

[a] Numbers in parentheses are estimated standard deviations of the last significant figures.

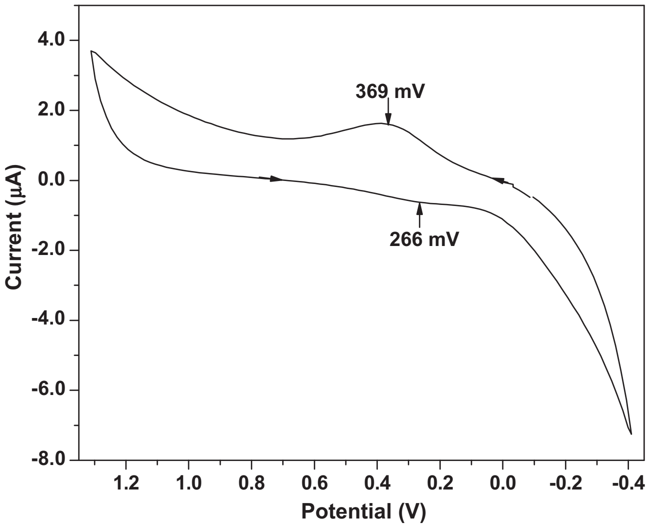

Fig. 5. Cyclic voltammogram for [Cu($O_2CAr^{4\text{-}FPh}$)$_2$(Hdmpz)$_2$] (**3**) in CH_2Cl_2 with 0.5 M $(Bu_4N)PF_6$ as supporting electrolyte and a scan rate of 100 mV/s.

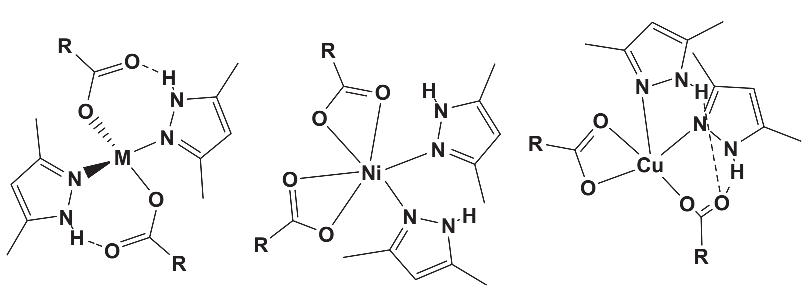

M = Fe and Co

2

3

Scheme 2. Variation of coordination geometries in the complexes.

4. Conclusion

In summary, use of the sterically-hindered 2,6-di-(*p*-fluorophenyl)benzoate and 3,5-dimethylpyrazole ligand afforded a series of mononuclear divalent transition metal complexes. Although compound **1**, **2**, **3** and $[Fe(O_2CAr^{4\text{-}FPh})_2(Hdmpz)_2]$ have identical ligand components, coordination geometry alters from tetrahedral to octahedral and square pyramidal depending on metal ion entity. It indicated that the geometry of coordination metal complexes is determined not only by the coordination environment but also by metal entity itself.

The ligands in metalloproteins are usually derived from amino acid side chain. The flexibility of such ligands is limited because the main chains with peptide bonds are localized in tertiary structures of enzymes. Thus, the coordination bonds between the metal ion and ligands from amino acid side chain may be severely restrained, resulting in the uncommon coordination geometry in the active site of metalloproteins often different from the small model complexes with synthetic ligands. In this work, however, due to the use of sterically hindered ligand, very uncommon coordination geometry could be modeled.

Acknowledgement

This work was supported partly by the Korea Science and Engineering Foundation (KOSEF) grant and the Converging Research Center Program through the National Research Foundation of Korea (NRF) (No. 2009-0082832) funded by the Korea government (MEST). This work was also supported in part by KIST (Korea Institute of Science & Technology) for 'National Agenda Project program', the faculty research program 2009 of Kookmin University in Korea and the Korea Science and Engineering Foundation (KOSEF) grant funded by the Korea government (MEST) (No. R11-2005-048-00000-0).

Appendix A. Supplementary data

CCDC 693438, 693439 and 695841 contains the supplementary crystallographic data for **1**, **2** and **3**. These data can be obtained free of charge via http://www.ccdc.cam.ac.uk/conts/retrieving.html, or from the Cambridge Crystallographic Data Centre, 12 Union Road, Cambridge CB2 1EZ, UK; fax: (+44) 1223-336-033; or e-mail: deposit@ccdc.cam.ac.uk. Supplementary data associated with this article can be found, in the online version, at doi:10.1016/j.poly.2010.10.019.

References

[1] R.L. Rardin, W.B. Tolman, S.J. Lippard, New J. Chem. 15 (1991) 417.
[2] H. Adams, S. Clunas, D.E. Fenton, S.E. Spey, Dalton Trans. (2002) 441.
[3] J. Kuzelka, J.R. Farrell, S.J. Lippard, Inorg. Chem. 42 (2003) 8652.
[4] Y. Tshuva, S.J. Lippard, Chem. Rev. 104 (2004) 987.
[5] A. Salifoglou, Coord. Chem. Rev. 228 (2002) 297.
[6] P. Lemoine, B. Viossat, G. Morgant, F.T. Greenaway, A. Tomas, N.H. Dung, J.J.R. Sorenson, J. Inorg. Biochem. 89 (2002) 18.
[7] R.L. Rardin, A. Bino, P. Poganiuch, W.B. Tolman, S. Liu, S.J. Lippard, Angew. Chem., Int. Ed. Engl. 129 (1990) 812.
[8] J.A. Ibers, R.H. Holm, Science 209 (1980) 223.
[9] H.A.O. Hill, Chem. Br. 1976 (1976) 119.
[10] H. Sigel (Ed.), Metal Ions in Biological Systems, Marcel Dekker, New York, 1998.
[11] R.J.P. Williams, in: J.J.R. Frausto de Silva (Ed.), The Natural Selection of the Chemical Elements: The Environment and Life's Chemistry, Oxford University Press, Oxford, 1996.
[12] J.J.R. Frausto de Silva, R.J.P. Williams, The Biological Chemistry of the Elements, Clarendon Press, Oxford, 1991.
[13] S.J. Lippard, J.M. Berg, Principal of Bioinorganic Chemistry, University Science Books, Mill Valley, CA, 1994.
[14] U.P. Singh, V. Aggarwal, A.K. Sharma, Inorg. Chim. Acta 360 (2007) 3226 (and references there in).
[15] M.A. Halcrow, Monocopper Oxygenases. Comprehensive Coordination Chemistry II, vol. 8, Elsevier, 2004. pp. 395–436.
[16] B.J. Barzeau, B.J. Johnson, C.M. Wilmot, Arch. Biochem. Biophys. 428 (2004) 22.
[17] J.P. Klinman, J. Biol. Chem. 281 (2006) 3013.
[18] A. Karmakar, R.J. Sarma, J.B. Baruah, Eur. J. Inorg. Chem. (2006) 4673.
[19] A. Karmakar, K. Deka, R.J. Sarma, J.B. Baruah, Inorg. Chem. Commun. 9 (2006) 836.
[20] R.N. Patel, N. Singh, V.L.N. Gundla, Polyhedron 26 (2007) 757.
[21] J. Ueda, T. Ozawa, M. Miyazaki, Y. Fujiwara, Inorg. Chim. Acta 214 (1993) 29.
[22] N. Cotelle, E. Tremolieres, J.L. Bernier, J.P. Catteau, J.P. Henichart, J. Inorg. Biochem. 46 (1992) 7.
[23] R.P. Hausinger, Biochemistry of Nickel, vol. 12, Plenum Press, New York, 1993. pp. 23–180.
[24] U.P. Singh, V. Aggarwal, S. Kashyap, S. Upreti, Transition Met. Chem. 34 (2009) 513.
[25] M. Dolores Santana, G. Garcia, G. Lopez, A. Lozano, C. Vicente, L. Garcia, J. Perez, Polyhedron 26 (2007) 1029 (and references there in).
[26] D. Lee, S.J. Lippard, J. Am. Chem. Soc. 120 (1998) 12153.
[27] J.R. Hagadorn, L. Que Jr., W.B. Tolman, J. Am. Chem. Soc. 120 (1998) 13531.
[28] J. Du Bois, T.J. Mizoguchi, S.J. Lippard, Coord. Chem. Rev. 200–202 (2000) 443.
[29] S. Yoon, S.J. Lippard, J. Am. Chem. Soc. 127 (2005) 8386 (and references there in).
[30] D. Lee, P.-L. Hung, B. Spingler, S.J. Lippard, Inorg. Chem. 41 (2002) 521.
[31] D.A. Dickie, G. Schatte, M.C. Jennings, H.A. Jenkins, S.Y.L. Khoo, J.A.C. Clyburne, Inorg. Chem. 45 (2006) 1646.
[32] D. Reger, A. Debreczeni, B. Reinecke, V. Rassolov, M.D. Smith, R.F. Semeniuc, Inorg. Chem. 48 (2009) 8911.
[33] C.-J.F. Du, H. Hart, K.-K. Daniel Ng, J. Org. Chem. 51 (1986) 3162.
[34] C.-T. Chen, J. Siegel, J. Am. Chem. Soc. 116 (1994) 5959.
[35] A. Saednya, H. Hart, Synthesis (1996) 1455.
[36] G.M. Sheldrick, Program Library for Structure Solution and Molecular Graphics: Version 6.2, Bruker AXS: Madison, WI, 2000.
[37] G.M. Sheldrick, SADABS: Area-Detector Absorption Correction, University of Gottingen, Gottingen, Germany, 2001.
[38] A.L. Spek, PLATON, A Multipurpose Crystallographic Tool, Utrecht University, Utrecht, The Netherlands, 2000.
[39] S. Trofimenko, Chem. Rev. 93 (1993) 943.
[40] M. Mohan, M.R. Bond, T. Otieno, C.J. Carrano, Inorg. Chem. 34 (1995) 1233.
[41] B. Machura, M. Jaworska, R. Kruszynski, Polyhedron 23 (2004) 2523.
[42] Y.-J. Sun, B. Zhao, P. Cheng, Inorg. Chem. Commun. 10 (2007) 583.
[43] M. Padmanabhan, S.M. Kumary, X.Y. Huang, J. Li, Inorg. Chim. Acta 358 (2005) 3537.
[44] K. Nakamoto, Infrared and Raman Spectra of Inorganic and Coordination Compounds, John Wiley and Sons, New York, 1986.
[45] M.P. Suh, Y.H. Oh, Bull. Kor. Chem. Soc. 3 (1982) 5.
[46] W.T. Lowther, D.A. McMillen, A.M. Orville, B.W. Matthews, Proc. Natl. Acad. Sci. USA 95 (1998) 12153.
[47] J.R. Hagadorn, L. Que Jr., W.B. Tolman, Inorg. Chem. 39 (2000) 6086.
[48] S.H. Kim, B.K. Park, Y.J. Song, S.M. Yu, H.G. Koo, E.Y. Kim, J.I. Poong, J.H. Lee, C. Kim, S.J. Kim, Y. Kim, Inorg. Chim. Acta 362 (2009) 4119.
[49] A.W. Addison, T.N. Rao, J. Reedijk, J. Van Rijn, G.C. Verchoor, J. Chem. Soc., Dalton Trans. (1984) 1349.
[50] S. Yoon, S.J. Lippard, J. Am. Chem. Soc. 126 (2004) 2666.